The MPGD-based Photon Detectors for the Upgrade of COMPASS RICH-1

M. Alexeev, C.D.R.Azevedo, R. Birsa, F. Bradamante, A. Bressan, M. Büchele, M. Chiosso, P. Ciliberti,
S. Dalla Torre, S. Dasgupta, O. Denisov, M. Finger, M. Finger Jr, H. Fischer , B. Gobbo, M. Gregori, G. Hamar,
F. Herrmann, S. Levorato, A. Maggiora, N. Makke, A. Martin, G. Menon, J. Novy, D. Panzieri, F. A. B. Pereira,
C. A. Santos, G. Sbrizzai, S. Schopferer, M. Slunecka, K. Steiger, L. Steiger, M. Sulc, F. Tessarotto and
J. F. C. A. Veloso

Abstract—The RICH-1 detector of the COMPASS Experiment at CERN SPS is undergoing an important upgrade: four new Photon Detectors, based on MPGD technology and covering a total active area larger than 1.4 m^2 will replace the MWPC-based photon detectors in order to cope with the challenging efficiency and stability requirements of the new COMPASS measurements. The new detector architecture consists in a hybrid MPGD combination: two layers of THGEMs, the first of which also acts as a reflective photocathode as it is coted with a CsI film, are coupled to a bulk Micromegas on a pad segmented anode; the signals are read-out via capacitive coupling by analog F-E based on the APV-25 chip. These detectors are the first application in an experiment of MPGD-based single photon detectors.

All aspects of the COMPASS RICH-1 Photon Detectors upgrade are presented and large emphasis is dedicated to the engineering aspects, the mass production and the quality assessment of the MPGD components. The status of the detector commissioning is also presented.

Index Terms—RICH; COMPASS; Photon detection; Micropattern gas detector; Thick GEM; Micromegas.

I. Introduction

THE RICH-1 detector [1] of the COMPASS Experiment [2] at CERN SPS is undergoing an important upgrade: four new Photon Detectors (unit size: 60×60 cm^2),

M. Alexeev is with the INFN Sezione di Torino, Torino, Italy and he is on leave from JINR, Dubna, Russia.

R. Birsa, S. Dalla Torre, B. Gobbo, M. Gregori, G. Hamar, S. Levorato, G. Menon, C. A. Santos and F. Tessarotto are with the INFN Sezione di Trieste, Trieste, Italy.

F. Bradamante, A. Bressan, P. Ciliberti, S. Dasgupta, N. Makke, A. Martin and G. Sbrizzai are with the INFN Sezione di Trieste and the University of Trieste, Trieste, Italy.

M. Chiosso is with the INFN Sezione di Torino and the University of Torino, Torino, Italy.

O. Denisov and A. Maggiora are with the INFN Sezione di Torino, Torino, Italy.

M. Finger, M. Finger Jr., J. Novy and M. Slunecka are with the Charles University, Prague, Czech Republic and JINR, Dubna, Russia.

M.Büchele, H. Fischer, F. Herrmann, and S. Schopferer, are with the Universität Freiburg, Physikalisches Institut, Freiburg, Germany.

K. Steiger, and L. Steiger are with INFN Sezione di Trieste, Trieste, Italy and the Technical University of Liberec, Liberec, Czech Republic, and their present address is Technical University of Liberec, Liberec, Czech Republic and Institute of Plasma Physics, Academy of Sciences of the Czech Republic, Turnov, Czech Republic.

D. Panzieri is with the INFN Sezione di Torino and the University of East Piemonte, Alessandria, Italy.

M. Sulc is with the Technical University of Liberec, Liberec, Czech Republic.

C.D.R.Azevedo, F. A. Pereira and J. F. C. A. Veloso are with Physics Department, University of Aveiro, Aveiro, Portugal.

based on MPGD technology and covering a total active area larger than 1.4 m^2 will replace the actual MWPC-based photon detectors in order to cope with the challenging efficiency and stability requirements of the new COMPASS measurements. In COMPASS RICH-1, MPGD photon detectors are used for the first time in a running experiment. This realization does not only represent an important achievement for the COMPASS experiment, but it also opens the way of a more extended use of novel gaseous photon detectors in the domain of the Cherenkov imaging technique for Particle IDentification (PID), key detectors in several research sectors and, in particular, in hadron physics. The relevance is related to the role of gaseous photon detectors, which are still the only available option to instrument detection surfaces when insensitivity to magnetic field, low material budget, and affordable costs in view of large detection surfaces are required. The MPGD-based photon detectors overcome the limitation of the previous generation of gaseous photon detector thanks to two essential performance characteristics: reduced ion backflow to the photocathode, namely reduced ageing and increased electrical stability, and faster signal development, namely higher rate capabilities.

II. The Novel Photon Detectors

The new detector architecture consists in a hybrid MPGD combination (Fig. 1): two layers of THick GEMs (THGEM) [3], the first of which also acts as a reflective photocathode (its top face is coated with a CsI film) are coupled to a MicroMegas (MM) [4] on a pad segmented anode; the signals are read-out via capacitive coupling. This architecture is the result of an eight-year R&D activity [5], whose central elements are:

- the exploration of the phase-space of the THGEM geometrical parameters;
- the development of the THGEM production technique;
- the introduction of the resistive MICROMEGAS by discrete elements and the optimization of the parameters of this original MICROMEGAS implementation.

Each of the four large hybrid 600×600 mm^2 single photon detectors is formed by two identical modules 600×300 mm^2, arranged side by side. The geometrical parameters of all the THGEM layers are: thickness of 470 μm, hole diameter of 400 μm and pitch of 800 μm. Holes are produced by mechanical drilling and have no rim, namely no uncoated area
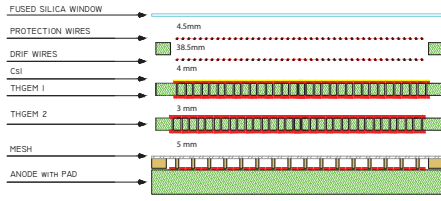
Fig. 1. Sketch of the hybrid single photon detector: two staggered THGEM layers are coupled to a bulk MicroMegas. The drift wire and protection plane are visible. Distances between the quartz window and between the electrodes are indicated too. Image not to scale.

Fig. 2. a) Sketch of the capacitive coupled readout pad. The biasing voltage is distributed via independent 470 MΩ resistors to the pad facing the micromesh structure. The buried pad is isolated via 70 μm thick fibreglass and connected to the front end chip. b) Schematic of the capacitive coupled pad principle illustrated via discrete elements blocks. c) Metallography section of the PCB: detail of the through-via contacting the external pad through the hole of the buried pad.

around the hole edge. The diameter of the holes located along the external borders have been enlarged to 500 μm in order to avoid an increased electric field in the peripheral THGEM holes. The top and bottom electrodes of each THGEM are segmented in 12 parallel areas separated by 0.7 mm clearance; the segments are grouped six by six forming two sectors per THGEM. The biasing voltage is individually provided to each sector of the THGEM. A fused silica window separates the radiator gas volume from the detector volume filled with Ar:CH$_4$ = 50:50 gas mixture. The protection wire plane is positioned 4.5 mm away from the window: it collects ions generated above the THGEMs to prevent their accumulation at the fused silica window. The drift wire plane (100 μm, 4 mm pitch), installed 4 mm from the CsI coated THGEM, is biased to a suitable voltage in order to maximize the extraction and collection of the converted photo-electron. The photo-electron is then guided into one of the first THGEM hole where the avalanche process is started due to the electric field generated by the biasing voltage applied between the top and bottom THGEM electrodes. The electron cloud generated in the first multiplication stage is then driven by the 1 kV/cm electric field across the 3 mm transfer region to the second THGEM, where thanks to the complete misalignment of the holes with respect to the first THGEM, the charge is distributed to several holes and it undergoes there a second independent multiplication process. Finally, the charge is guided by the 0.8 kV/cm field across the 5 mm gap to the MM where the last multiplication occurs. The MMs have a gap of 128 μm; they are built using MM bulk technology [6] using 300 μm diameter pillars with 2 mm pitch. The intrinsic ion blocking capabilities of the MicroMegas as well as the arrangements of the THGEM geometry and fields grants an ion back flow to the photocathode surface lower or equal to 4%. The charge is collected by the 7.5×7.5 mm^2 pad segmented anode biased at positive voltage and facing the grounded micromesh. This segmentation results in 4760 readout channels per detector. Each pad is biased trough an independent resistor and the signal, induced on the parallel buried pad (Fig. 2), is read out by the Front End APV 25 chip [7]. The 500 μm clearance between pads prevents the discharge, when occurring, to propagate towards the surrounding pads: the voltage drop of the anodic pads surrounding a tripping one is about 2 V over the 620 V operation voltage, causing a local gain drop lower
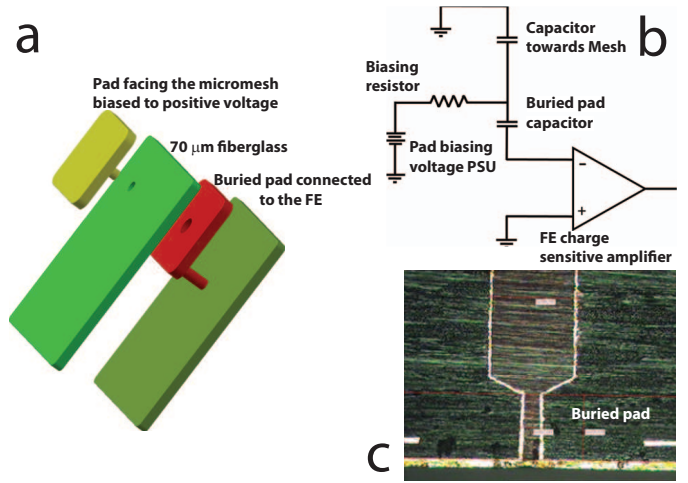
than 4%. The nominal voltage condition of the tripped pad is restored in about 20 μs. The THGEM correct position and planarity is guaranteed by 12 pillars by Peek glued onto corresponding pillars by photosensitive material present in the MM layer.

III. CONSTRUCTION, QUALITY CONTROL OF THE COMPONENTS, DETECTOR ASSEMBLY AND INSTALLATION

Quality control tools, methods and protocol have been developed as well. They include:

- preselection of the row material for the PCB that will form the THGEMs in order to use only foils with homogeneous thickness to guarantee the homogeneity of the gain;
- THGEM control by optical inspection, by collecting and analyzing microscope images scanning by samples the large multiplier surface;
- THGEM validation by gain maps using the multipliers in single layer detectors;
- THGEM validation by measuring the breakdown voltage in nitrogen and comparing it with the phenomenological Paschen limit [8];
- MICROMEGAS stability and gain maps illuminating the detectors by an X-ray gun station;
- Measurement of the quantum efficiency of the CsI photocathodes;
- Gas leak checks and overall electrical stability checks of the final detectors.

The detector design, including its mechanical components, is compatible with the RICH-1 detectors of the central region, namely MultiAnode PhotoMultiplier Tubes (MAPMT) coupled to individual lens telescopes that equip the central RICH region and that remain unchanged. Due to the CsI coating on the first THGEM the whole set of assembly and

installation operations had to be performed in an air free atmosphere, i.e. a glove box flushed with N_2, as well as the detector transportation and final installation on the RICH-1. The installation was completed by May 2016. Construction and installation have been intense activities that required about 11.5 man-year over the last year of the project completion.

IV. THE HIGH VOLTAGE CONTROL SYSTEM

An essential tool for the detector commissioning is the high voltage control system, which also grants the voltage and current monitoring and data recording. The power supplies are commercial ones by CAEN [1] inserted in a SY4527 mainframe. The four detectors are organized, from the HV supply point of view, in four independent sectors each; nine different electrode types, each one with its specific role, are present in the multilayer detectors. Manual setting and control of all these HV channel would be both unsafe and unpractical.

The voltages and currents of all the channels are read-out and recorded at 1 Hz frequency. If the current spark rate is above a given value the voltage is automatically readjusted.

V. COMMISSIONING AND PERFORMANCE FIGURES

So far, the detectors have operated stably for five months. Two out of the four detectors present a large electronic noise affecting about 25% of the detector channels: the cause of the anomalous noise level has been identified in an incorrect routing of the grounding. The intervention to fix the grounding has been postponed to the 2016-17 winter shutdown not to interfere with the 2016 COMPASS data taking . The other two detectors present a noise level lower than 1000 ENC.

The performance, in terms of voltage stability of the MM can be observed in Fig. 3 a) where the current and voltage values of a MM are plotted for a time range of ten days. No sizeable voltage drop is observed when a current speak occurs, confirming the validity of the detector design. In Fig. 3 b) a zoomed view of the voltage curve is shown where the slow continuous voltage modulation is the effect of the correction applied by the high voltage control system to compensate for the evolution of the environment parameters, namely pressure and temperature, in order to preserve the stability of the detector gain. The single photon amplitude spectra collected changing only the biasing voltages of the two THGEM set at the values of 1250, 1275 and 1300 V are shown in Fig. 4 a). Similarly in Fig. 4 b) where only the biasing voltage of the MM is set at the voltage values of 588, 600, 612, 624 V. The gain values of the spectra shown in fig. 4 range between 12k and 25k. The different slopes of the exponential distributions are in agreement with the expected values from the laboratory exercises and they confirm the good detector response.

A preliminary relative comparison between the hybrid photon detectors and the MWPC, the ones which have not been replaced, is performed by counting the number of detected photons and correcting them for the different geometrical acceptance of the detectors under study. From this simple estimate obtained analyzing the same data set, it is possible

[1]CAEN - Costruzioni Apparecchiature Elettroniche Nucleari S.p.A., Via della Vetraia, 11, 55049 Viareggio LU, Italy
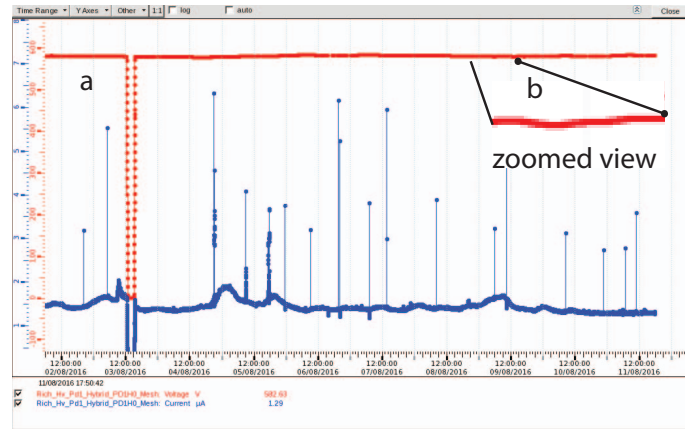

Fig. 3.   a) Voltage an current monitored for one of the hybrid bulk MicroMegas by the Hybrid HV control System for a time range of 10 days. b) Zoomed view of the voltage curve:the corrections applied by the voltage control system to compensate for pressure and temperature variations are evident.
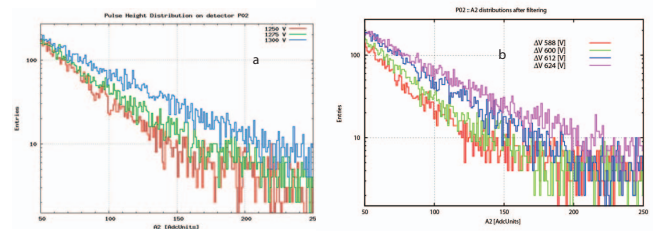

Fig. 4.   a) Amplitude distribution of the single photon signal collected for different biasing voltages of the THGEM electrode: 1250, 1275,1300 V. b) Amplitude distribution of the single photon signal collected for different biasing voltages of the MM electrode: 588, 600, 612, 624 V.

to conclude that the photon detection efficiency of the hybrid detectors is larger than that of the MWPC.

The detector commissioning and characterization is on-going. The preliminary indications reported here allow to conclude that the novel detectors will be able to satisfy the COMPASS RICH-1 requirements.

REFERENCES

[1] E. Albrecht, et al., Nucl. Instr. and Meth. A 553 (2005) 215; P. Abbon et al., Nucl. Instr. and Meth. A 587 (2008) 371; P. Abbon et al., Nucl. Instr. and Meth. A 616 (2010) 21; P. Abbon et al., Nucl. Instr. and Meth. A 631 (2011) 26.
[2] The COMPASS Collaboration, P. Abbon et al., Nucl. Instr. and Meth. A 577 (2007) 455; the COMPASS Collaboration, P. Abbon et al., Nucl. Instr. and Meth. A 779 (2015) 69.
[3] L. Periale et al., Nucl. Instr. and Meth. A 478 (2002) 377; P. Jeanneret, PhD thesis, Neuchatel University, 2001; P.S. Barbeau et al, IEEE NS-50 (2003) 1285; R. Chechik et al, Nucl. Instr. and Meth. A 535 (2004) 303.

[4] Y. Giomataris et al., Nucl. Instr. and Meth. A 376 (1996) 29; G. Charpak et al., Nucl. Instr. and Meth. A 412(1998)47; G. Barrouch et al., Nucl. Instr. and Meth. A 423 (1999)32.

[5] M. Alexeev et al., Nucl. Instr. and Meth. A 610 (2009) 174; M. Alexeev et al., Nucl. Instr. and Meth. A 617 (2010) 396; M. Alexeev et al., Nucl. Instr. and Meth. A 623 (2010) 129; M. Alexeev et al., 2010 JINST 5 P03009; M. Alexeev et al., Nucl. Instr. and Meth. A 639 (2011) 130; M. Alexeev et al., 2012 JINST 7 C02014; M. Alexeev et al., Nucl. Instr. and Meth. A 695 (2012) 159 M. Alexeev et al., 2012 JINST 7 C002014; M. Alexeev et al., Physics Procedia, 37 (2012) 781; M. Alexeev et al., Nucl. Instr. and Meth. A 732 (2013) 264; M. Alexeev et al., 2013 JINST 8 P01021; M. Alexeev et al., 2013 JINST 8 C12005; M. Alexeev et al., 2014 JINST 9 C03046; M. Alexeev et al., 2014 JINST 9 P01006; M. Alexeev et al., 2014 JINST 9 C09017; M. Alexeev et al., Nucl. Instr. Meth. A 766 (2014) 133; M. Alexeev et al., Nucl. Instr. Meth. A 766 (2014) 199; M. Alexeev et al., Nucl. Instr. Meth. A 766 (2014) 208; F. Tessarotto et al., 2014 JINST 9 C09011; M. Alexeev et al., PoS (TIPP2014) 075; M. Alexeev et al., 2015 JINST 10 P03026; M. Alexeev et al., Nucl. Instr. Meth. A 824 (2016) 139.

[6] I. Giomataris et al., Nucl. Instr. and Meth. A 560 (2006) 405.

[7] M.J. French, et al., Nucl. Instr. and Meth. A 466 (2001) 359.

[8] F. Paschen, Annalen der Physik 273 (1889) 69.